

Circular patch planar ultra-wideband antenna for 5G sub-6 GHz wireless communication applications

R. AZIM^{a,*}, R. AKTAR^a, A. K. M. M. H. SIDDIQUE^a, L. C. PAUL^b, M. T. ISLAM^c

^aDepartment of Physics, University of Chittagong, Chittagong 4331, Bangladesh

^bDepartment of EECE, Pabna University of Science and Technology, Pabna 6600, Bangladesh

^cDepartment of Electrical, Electronic & Systems Engineering, Faculty of Engineering and Built Environment, Universiti Kebangsaan Malaysia, 43600 Bangi, Malaysia

This paper presents a circular patch planar ultra-wideband antenna for sub-6 GHz 5G communication applications. The anticipated antenna is composed of a circular patch and a ground plane and no lumped element or large system ground plane is required. To achieve the desire operating band, a rectangular slot has been inserted at the top edge of the ground plane. The measured results demonstrate that, the operating band of the studied antenna is ranging from 3.05 to 5.82 GHz with $S_{11} \leq -10\text{dB}$, covering the entire N77/N78/N79 band for sub-6 GHz 5G as well as LTE, WiMAX and WLAN wireless communication system. The studied antenna has a good gain, efficiency and demonstrates stable omnidirectional radiation characteristics. Due to its distinctive characteristics such as planar profile, small footprint, symmetric radiation behaviour and good gain, the studied antenna could be a promising competitor to be used in 5G and existing wireless communication services.

(Received April 30, 2020; accepted April 8, 2021)

Keywords: Antenna, 5G, Circular patch, Planar, LTE, Sub-6 GHz

1. Introduction

Due to the growing need of data-hungry devices and smart phone applications, the information flow in mobile wireless communication is almost doubled every year. It is expected that by the year 2021, mobile phones numbers (5.5 billion) will be higher than the landline numbers (2.9 billion) or bank accounts (5.4 billion) [1]. To fulfil the increasing demand, the fifth generation (5G) mobile communication system is already deployed in different countries of the world [2]. In 2019, the numbers of 5G mobile connections was 5 million which is expected to be 577 million by the year 2023 [3]. Compared to the current generations, 5G wireless communications is characterised with distinctive metrics including a data transmission rate of Gbps, a latency time of millisecond, a very high traffic volume density, ultra-dense connections, enhanced spectral energy, and cost effectiveness [4]. The ITU has allocated the following spectrum for 5G communications, including the 3.4-3.6 GHz, 5-6 GHz, 24.25-27.5 GHz, 37-40.5 GHz, and 66-76 GHz bands [5], and the FCC has authorized the spectrum of 27.5-28.35 GHz for 5G. Usually at high frequency (mmWave) bands, the EM wave facing difficulties of signal fading, severe path loss and atmospheric absorptions results in the degradation of signal-to-interference-plus noise ratio. Service providers are using the existing base stations sites meant for the sub-6 GHz frequency band for smooth and easier implementation of 5G. It is therefore thought that frequency spectrum below 6 GHz also known as sub-6 GHz band serves as the primary frequency band for the commissioning of the 5G, especially for the N77 (3.3-4.2 GHz), N78 (3.3-3.8 GHz) and N79 (4.4 - 5.0 GHz) bands

[6]. Currently, the 3.4-3.8 GHz band, which is the combination of LTE band 42 (3.4-3.6 GHz) and LTE band 43 (3.6-3.8 MHz) has been authorized by many countries including European Union, China, South Korea, Japan, USA as a pioneer to get on the 5G [6-7]

Antennas are the key component in any wireless communication that establishes the link between transmitter and receiver. As the 5G communication system has been implemented in different countries of the World, antenna design for 5G base stations and mobile phones is therefore be in great demand [8]. To achieve the fastest 5G services, the designed antenna should exhibit multiple resonance modes to cover the whole 5G sub-6 GHz band. Therefore, it is highly desirable to design an antenna with wideband performance to fully cover all the sub-6 GHz 5G bands as well as existing 4G long term evolution (LTE) bands. A suitable 5G antenna must be small enough to be compatible to the portable wireless devices. Low-profile planar antenna and compatibility for integration with printed circuit board is also highly desirable for easy embedding into wireless devices.

Different techniques and methods have already been reported to design planar antenna for 5G applications [9-19]. For railway communication system in [9], an antenna for 3.5 GHz 5G applications is presented. To attain desire operating band, the proposed design employ an elliptical shaped patch. However, it has a large size of $60 \times 180 \text{ mm}^2$. In [10], a dipole antenna that achieved dual operating bands of 1.24-2.64 GHz and 3.34-5 GHz is presented. However, it fabricated on a large ground plane of $80 \times 150 \text{ mm}^2$. A broadband planar antenna that operates over 3.4-5.5 GHz band is presented in [11]. But it possesses a large volumetric size of $120 \times 60 \text{ mm}^2$ and

requires a balun structure to feed the antenna. Without using any 3D structure and lumped elements, in [12] a planar antenna is reported for 5G mobile terminal. The antenna consists of one multi-branch driven strip and three parasitic ground strips and able to operate over 700 - 960 MHz and 1.6-5.5 GHz ($S_{11} \leq -6\text{dB}$). However, it needs a large ground plane of $80 \times 135 \text{ mm}^2$. An antenna that operates over 2.32-5.24 GHz band is presented in [13]. In this design the ground plane is modifying and changed to step-impedance resonator to achieve the desired operating band to cover sub-6 GHz. For 4G and sub-6 GHz 5G base station applications, a cross dipole antenna is reported in [14]. With an overall dimension of $76 \times 42 \text{ mm}^2$, the single element of the designed antenna attained an operating band of 1.341-3.834 GHz. In [15], a planar antenna is reported for numerous wireless communication applications. The antenna is comprised of a T-shaped patch and partial ground plane and fabricated on epoxy-resin material. The antenna achieved an operating bandwidth of 1.54 GHz ranging from 2.02 to 3.56 GHz. The antennas reported in [16-18] possess large volumetric size, complex design and fail to cover the entire sub-6 GHz 5G band. Moreover, their three dimensional structure limits their uses in handheld devices. Many reported 5G antennas either have large size or do not achieved required operating band to cover the sub-6 GHz 5G band. Moreover, change of the electrical length of antennas with the frequency results in a remarkable deterioration in the radiation patterns which possess a challenge to design new antennas for 5G sub-6 GHz band.

In this paper a simple circular patch ultra-wideband planar antenna for sub-6 GHz 5G mobile communication is presented. The presented design possesses a fully planar structure and no lumped elements or large system ground plane are required. Moreover, it has a small volumetric size of $20 \times 28 \times 1.6 \text{ mm}^3$ on the FR4 substrate material which is much smaller than many antennas reported for the same applications. The anticipated antenna is simulated, prototyped and tested. Measured result shows that the circular patch matched well with the ground plane and the studied antenna managed to work over the 3.05-3.82 GHz ($S_{11} \leq -10\text{dB}$) band and is able to cover all sub-6 GHz bands as well as popular narrow-service bands of WiMAX, WLAN and LTE bands of 42, 43 and 46.

Table 1. Proposed antenna specification with different parameters

Parameters	Values (mm)	Descriptions
W	20	Width of the substrate
L	28	Length of the substrate
R	7	Radius of the circular patch
L_G	14	Length of the ground plane
L_f	14.15	Length of the feedline
W_f	3	Width of the feedline
W_S	14	Width of the slot
L_S	3	Length of the slot
W_l	3	Width of the vertical edges
h	1.6	Height of the substrate

2. Antenna design

2.1. Antenna geometry

The circular patch and planar profile is chosen for the design of proposed antenna. Circular and rectangular patch structures are the simplest antenna structure. The planar structure of the anticipated antenna is chosen due to their distinctive features of light weight, inexpensive, ease of fabrication, low profile, compatibility with integrated circuits, variable structure for exciting broad impedance bandwidths and symmetric radiation behaviours. In the study of the presented antenna, transmission line model is used to determine the radius of the circular patch. According to this model the radius of the circular microstrip patch can be written as [20]

$$R = \frac{f}{\left\{1 + \frac{2h}{\pi \epsilon_r f} \left[\ln \left(\frac{\pi f}{2h} \right) + 1.7726 \right] \right\}^{\frac{1}{2}}} \quad (1)$$

The patch electrically looks larger compared to its physical dimensions due to the adjoining field around the boundary of the patch. The effective radius of the patch can be calculated using [20]

$$R_e = R \left[1 + \frac{2h}{\pi R \epsilon_r} \left(\ln \frac{\pi R}{2h} + 1.7726 \right) \right]^{\frac{1}{2}} \quad (2)$$

where

R_e = the effective radius due to fringing field

h = thickness of the substrate

ϵ_r = dielectric constant of the substrate

f = central frequency

The antenna is solely targeted to operate over sub-6 GHz 5G bands (3-5 GHz). To attain the desired performances, the design necessities such as dielectric constant and bandwidth are subsequently adjusted to achieve the most desirable size of the patch using CST microwave studio simulator.

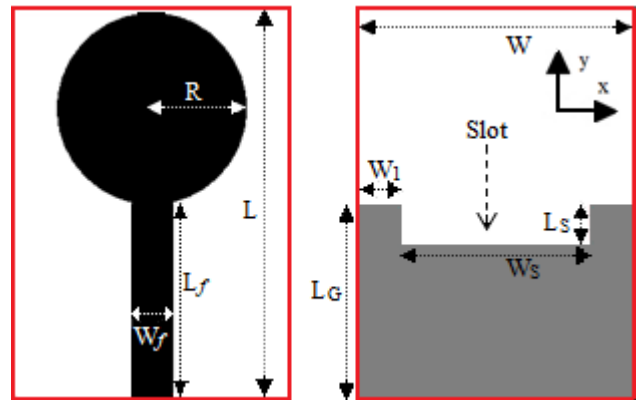


Fig. 1. Geometry of the proposed antenna (a) top view (b) bottom view (color online)

The geometric layout of the anticipated antenna is displayed in Fig. 1. The antenna made up of a microstrip line fed circular shaped patch and a ground plane. R denotes the radius of the patch and the etched ground plane has a dimension of $W \times L_G$. The width and length of the feedline are respectively chosen as W_f and L_f to achieve 50Ω characteristic impedance. The patch and the feedline is etched on the top side of a FR4 substrate of thickness 1.6 mm, relative permittivity 4.6 and loss tangent 0.02 while the ground plane is designed on the bottom side. To increase the impedance matching, a slot of size $W_S \times L_S$ has been inserted on the ground plane. The antenna has an overall size of $W \times L$. After a comprehensive parametric study, it is found that the proposed antenna has the optimized design parameters as summaries in the Table 1.

2.2. Parametric study

To design the proposed sub-6 GHz 5G antenna, an extensive parametric research is conducted. The study is very necessary since it offers some understanding of antenna performances for an antenna engineer. The effects of varying the ground plane length (L_G), radius of the circular patch (R), and width of the feedline (W_f) are studied. During the study, except for the parameter of interest, the other parameters remained unaltered. The size of the ground plane is very sensitive parameter in the designing of ultra-wideband antenna. Different researchers have observed the strong dependence of operating bandwidth on the ground plane size [21 - 23]. The simulated S_{11} for different values of ground plane length, L_G (without and with slot) are depicted in Fig. 2(a). It is clear to see from the figure that the operating bandwidth is strongly dependent on L_G . Decreasing and increasing the values of L_G from a certain value reduces the impedance-matching, results in a reduction of operating bandwidth. To improve the impedance matching and to make the design compact, a rectangular slot of $14 \times 3 \text{ mm}^2$ is etched at the top middle edge of the ground plane. As the slot increases the gap between patch and ground plane, the impedance matching is improved due to extra electromagnetic coupling between them. It can be observed from the Fig. 2(a) that $L_G = 14 \text{ mm}$ with a slot on its top middle edge can maintain good operating bandwidth with lowest S_{11} .

Fig. 2(b) presented the change of S-parameter with patch radius (R). It can be seen that decreasing and increasing the values of R from the optimized one increases the mismatch between the patch and ground plane results in an overall decrement of impedance bandwidth. In the proposed antenna, a radius of 7 mm is taken as the final value.

Fig. 2(c) demonstrates the simulated S_{11} with different values feedline width, W_f ($W_f = 1, 3, \text{ and } 5 \text{ mm}$). As the feedline act as an impedance matching circuit, the width of the feedline can change the input impedance of the studied antenna, results in a variation in the operating band. It can be seen that a width of 3 mm can demonstrates the best S_{11} value within the operating band.

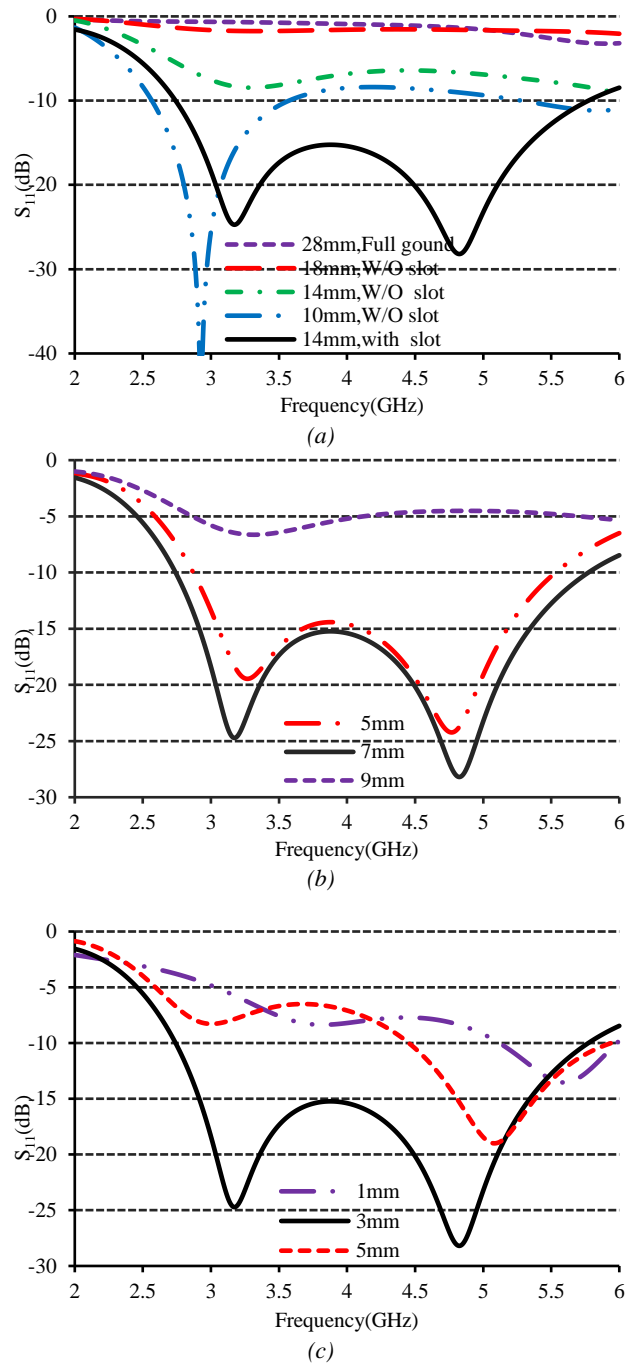


Fig. 2. Simulated S-parameters for different values of (a) L_G (W/O and with slot) (b) R , and (c) W_f . (color online)

3. Experimental results and discussion

To verify the performances, a prototype of the studied antenna is fabricated and is shown in Fig. 3. The input impedance characteristics of the prototype has been measured using N5227A PNA network analyzer. Fig. 4 displayed the measured S_{11} of the designed antenna along with the simulated one where a fair agreement has been observed. The measured result in the plot confirm that the presented antenna is able to achieve a bandwidth of 2.77

GHz (3.05 - 5.82 GHz, 62.46%). Slight disagreements between the two results is mainly due to fabrication errors and imperfect soldering. Moreover, it can be due to the effect of feeding cable used during the measurement. In spite of its small size, the studied antenna is able to work over a wide operating band covering the all sub-6 GHz band assigned for mid 5G communication applications as well as existing LTE bands, WiMAX and WLAN.



Fig. 3. Top (left) and bottom (right) view of the prototype (color online)

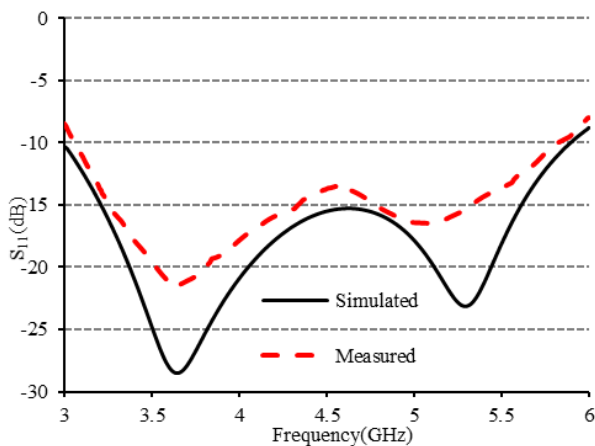


Fig. 4. Simulated and measured S_{11} (color online)

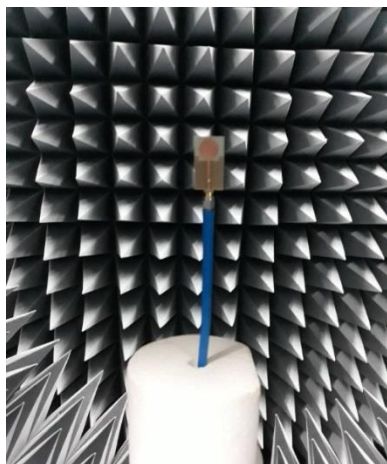


Fig. 5. Radiation characteristics measurement set-up in StarLab (color online)

The radiation characteristics of the studied antenna are measured using StarLab 0.6 - 18 GHz anechoic chamber from MVG as shown in Fig. 5 [24]. The StarLab uses the near-field measurement techniques that allow the measurement of electric fields to calculate the corresponding far-field data of the antenna under test. The measured peak gain of the prototyped antenna in the operating band is displayed in Fig. 6. It can be observed from the plot that in the operating band the studied antenna achieved an average gain of 0.34 dBi with a maximum of 4.21 dBi. The measured efficiency of the fabricated antenna is presented in Fig. 7. The plot shows that the maximum efficiency is 87.13 % with an average of 65.35 %. As the antenna is prototyped on standard FR4 substrate, the dielectric loss is high, which affect the gain as well as efficiency. These low gain and efficiency of the studied antenna could be improved using a loss-free dielectric material.

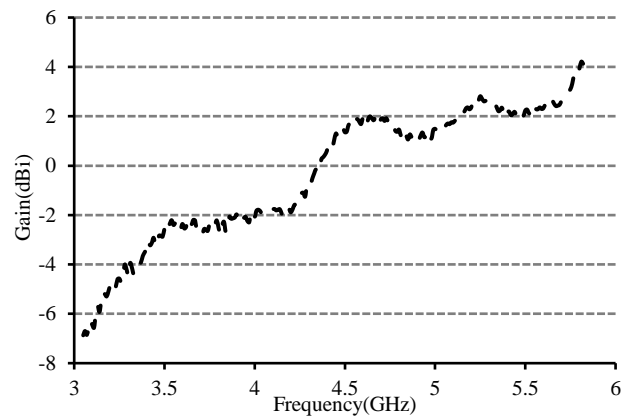


Fig. 6. Measured peak gain of the proposed antenna

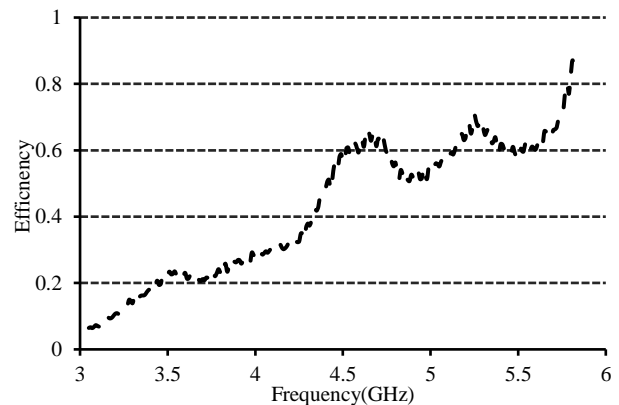


Fig. 7. Measured efficiency of the proposed antenna

The simulated current distributions on the studied antenna at resonance frequencies of 3.2 and 4.8 GHz are displayed in Fig. 8, and the measured radiation patterns at these frequencies in the E - and H -planes are shown in Fig. 9. In the radiation pattern plot, the solid line represents the co-polarized field (E_{θ}) whereas the dashes line represents the cross-polarized field (E_{ϕ}). Through a simulation study of the current distributions on the antenna, two characteristics current modes are found to exist over the operating band from 2 to 6 GHz. These two current modes

are dominant at resonance frequencies of 3.2 and 4.8 GHz respectively. At the first resonance frequency of 3.2 GHz, Fig 8(a) shows that the current is uniformly distributed on the patch, hence, the radiation pattern in both the E - and H -planes as shown in Fig. 9(a) are almost omnidirectional and are roughly similar to that of typical monopole antennas. At the higher frequency of 4.8 GHz, higher order current modes are excited, and the surface current is less

evenly distributed on the patch as displayed in Fig. 8(b). The radiation patterns, as can be observed in Fig. 9(b) become slightly directional with some nulls in the bore-site directions. Despite these nulls, the plots in Fig. 9 show that the radiation patterns of the studied antenna are symmetric all over the operating band.

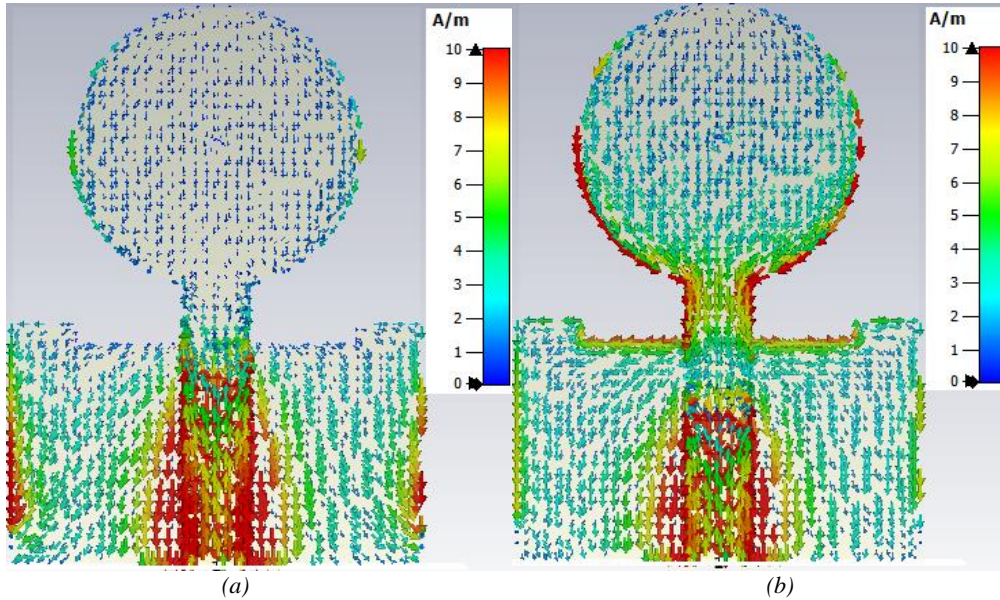


Fig. 8. Current distributions at (a) 3.2 and (b) 4.8 GHz (color online)

Table 2. Comparison of proposed antenna with previous works

Design	Ref.	Size***	Bandwidth	Antenna Structure	Peak Gain
1	[9]**	$0.66\lambda_0 \times 1.97\lambda_0$	0.50 GHz	Double layer patch	6.1 dBi
2	[10]	$0.89\lambda_0 \times 1.67\lambda_0$	1.66 GHz (-6dB)	Single layer with large system ground plane	6.0 dBi
3	[11]	$0.68\lambda_0 \times 1.36\lambda_0$	2.1 GHz	Single layer patch with balun and reflector	5.8 dBi
4	[12]**	$0.43\lambda_0 \times 0.72\lambda_0$	3.9 GHz (-6dB)	Single layer with large system ground plane	4.7 dBi
5	[13]	$0.39\lambda_0 \times 0.62\lambda_0$	2.92 GHz	Single layer patch with step impedance resonator	4.31 dBi
6	[14]	$0.34\lambda_0 \times 0.19\lambda_0$	2.493 GHz	Single layer patch with dipole and balun structure	3.2 dBi
7	This work	$0.20\lambda_0 \times 0.28\lambda_0$	2.77 GHz	Single layer patch	2.45 dBi

**Only sub-6 GHz band is considered for comparison.

*** λ_0 corresponds to the lowest frequency of the operating band.

In Table 2, the performance of the studied antenna is compared with some previous antennas. It is clear to see that the proposed antenna occupies a very small area to achieve comparable or even wider operating band as compared with antennas presented in [9 - 14]. Unlike the antennas presented in [10, 12 -13], no large system ground plane or reflector [11] are necessary in the present design, which lessen the fabrication difficulties. Furthermore, the prototyping of the studied antenna is much easier than the

antenna reported in [14], since the studied antenna possesses fully planar structure and no dipole element or balun structure is necessary. Hence, the studied antenna has advantages of wide operating band, small size, and ease of fabrication, which makes it suitable for sub-6 GHz 5G communication applications.

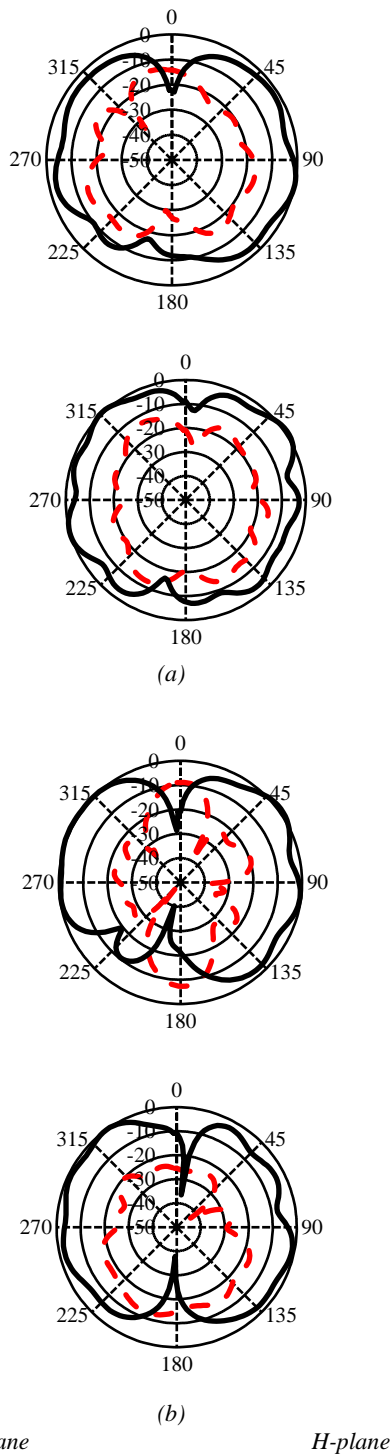


Fig. 9. Measured radiation patterns at (a) 3.2 GHz, and (b) 4.8 GHz. The solid black lines represent the co-polarized component and dashes red lines represent the cross-polarized component (color online)

4. Conclusions

In this paper, a low-profile antenna is presented for sub-6 GHz 5G communication applications. The presented antenna consist of circular patch and ground plane has a fully planar structure and no lumped elements or large

system ground plane are required, which makes it a simple structure and easy of fabrication. The measured -10dB bandwidth of the fabricated antenna is ranged from 3.05 to 5.82 GHz covering LTE band 42, LTE band 43, LTE band 46, WiMAX 3.5 GHz, WLAN 5.2 GHz, WiMAX 5.5 and WLAN 5.8 GHz and N77/78/79 bands for 5G communication applications. The antenna also achieved good gain, efficiency and exhibits stable radiation behaviour. The prime advantage of the studied antenna is its capability to cover newly introduced 5G sub-6 GHz bands as well as existing WiMAX, WLAN and 4G LTE bands.

Acknowledgments

The authors would like to thank the University of Chittagong, Bangladesh to sponsor this work under the grant number 246(17)/P&D/7-37(2)/2nd/2019.

References

- [1] Cisco Systems. Mobile Visual Networking Index (VNI) Forecast Project 7-Fold Increase in Global Mobile Data Traffic from 2016 - 2021. <https://newsroom.cisco.com/press-release-content?articleId=1819296>
- [2] Qualcomm, <https://qualcomm.com/media/documents/files/spectrum-for-4g-and-5g.pdf>.
- [3] Strategy Analytics, <https://strategyanalytics.com/strategy-analytics/news/strategy-analytics-press-releases/2018/03/27/strategy-analytics-forecasts-nearly-600-million-5g-users-by-2023>.
- [4] S. Chen, J. Zhao, IEEE Commun. Mag. **52**(5), 36 (2014).
- [5] International Telecommunication Union, https://itu.int/en/ITU-D/Regulatory-Market/Documents/Events2019/Togo/5G-Ws/Ses4_Joaquin_Spectrum-5G.pdf.
- [6] M. Agiwal, A. Roy, N. Saxena, IEEE Commun. Surveys Tuts **18**(3), 1617 (2016).
- [7] GSM Association (GSMA), 5G Spectrum Public Policy Position, White Paper, November 2016. https://www.gsma.com/iot/wp-content/uploads/2016/08/GSMA-5G-Spectrum-PPP_eng.pdf
- [8] H.-C. Huang, Proceeding of the 2018 International Workshop on Antenna Technology, China, 1 (2018).
- [9] A. K. Arya, S. J. Kim, S. Kim, Prog. Electromagn. Res. Lett. **88**, 113 (2020).
- [10] M. Khalifa, L. Khashan, H. Badawy, F. Ibrahim, J. Phys. Conf. Ser. **1447**, 6588 (2020).
- [11] K. M. K. H. Leong, Y. Qian, T. Itoh, IEEE Microw. Wireless Compon. Lett. **11**(2), 62 (2001).
- [12] Z. An, M. He, Appl. Comput. Electromagn. Soc. J. **35**(1), 10 (2020).
- [13] X. Tang, Y. Jiao, H. Li, W. Zong, Z. Yao, F. Shan, Y. Li, W. Yue, S. Gao, Proc. iWEM 2019, Qingdao,

- China, 18 - 20 September 2019.
- [14] G. Gopal, A. Thangakalai, *Appl. Comput. Electromagn. Soc. J.* **35**(1), 16 (2020).
- [15] R. Azim, K. Dhar, M. M. Alam, M. T. Islam, *Optoelectron. Adv. Mat.* **14**(11-12), 509 (2020).
- [16] J-N. Sun, J-L. Li, L. Xia, *IEEE Access* **7**, 161708 (2019).
- [17] G. Jin, C. Deng, J. Yang, Y. Xu, S. Liao, *IEEE Access* **7**, 56539 (2019).
- [18] J. Guo, Y. Zou, C. Liu, *IEEE Antennas Wireless Propag. Lett.* **10**, 435 (2011).
- [19] A. Affandi, R. Azim, M. M. Alam, M. T. Islam, *Electronics* **9**(3), 393 (2020).
- [20] G. Ramesh, B., Prakash, J. B. Inder, A Ittipiboon, *Microstrip Antenna Design Handbook*, Artech House Publishers, Norwood, Massachusetts, USA 2001.
- [21] R. Azim, M. T. Islam, N. Misran, *Appl. Comput. Electromagn. Soc. J.* **26**(10), 856 (2011).
- [22] R. Azim, M. T. Islam, N. Misran, *Arab. J. Sci. Eng.* **38**(9), 2415 (2013).
- [23] R. Azim, K. Dhar, M. M. Alam, M. T. Islam, *Optoelectron. Adv. Mat.* **14**(11-12), 509 (2020).
- [24] Microwave Vision Group, StarLab, <https://www.microwavevision.com>.

* Corresponding author: rezaulazim@cu.ac.bd